JUNE 1982 LRP 208/82

NONLINEAR EFFECTS IN A BEAM PLASMA SYSTEM : SECOND HARMONIC EMISSION AND DENSITY DEPRESSION FORMATION

J.A. Michel, P.J. Paris, M. Schneider and M.Q. Tran

Invited paper at the Chalmers Symposium on Plasma Physics, Aspenäsgården, June 16-18, 1982

To be published in Physica Scripta

NONLINEAR EFFECTS IN A BEAM PLASMA SYSTEM: SECOND HARMONIC EMISSION AND DENSITY DEPRESSION FORMATION

J.A. Michel, P.J. Paris, M. Schneider and M.Q. Tran

Centre de Recherches en Physique des Plasmas, Association Euratom - Confédération Suisse, Ecole Polytechnique Fédérale de Lausanne, 21, Av. des Bains, CH-1007 Lausanne, Switzerland

ABSTRACT

The nonlinear evolution of Langmuir waves excited by the beam-plasma instability is studied experimentally. The emission of electromagnetic waves at the second harmonic of the plasma frequency and the formation of a density depression have been observed. These phenomena are consistent with the predictions of the strong Langmuir turbulence theory.

1. INTRODUCTION

Electromagnetic wave emission was first observed by astrophysicists more than thirty years ago. In the solar system, radio emission occurs in a sporadic way and is correlated with solar flares[1]. Type III solar bursts have received persistent interest due to their properties and the associated theoretical problem. Let us recall the salient characteristics of type III bursts [1, 2, 3, 4]. Type III bursts are emitted in two frequency bands, one around the local plasma frequency ω_{pe} and the second one around twice ω_{pe}: the power emitted in each band is comparable. The electromagnetic emission is associated with an energetic electron beam ($E_b \sim 20 - 100$ keV) emitted during a solar flare. Satellite observations show that the beam propagates at least one A.U. Observations at one A.U. indicate that second harmonic emissions are correlated with arrival of the energetic electron beam [5]. The observation of the electron beam at a distance so far from its source (the sun) raises the question of beam stabilization. Quasi-linear effects lead to a very strong coupling between the beam and the unstable Langmuir wave: the electron beam would then be stabilized in the solar corona itself [6]. Both effects (i.e., second harmonic emission and beam propagation) can be explained by the strong Langmuir turbulence theory [4, 7-14]. The source of the second harmonic electromagnetic waves is the nonlinear current associated with the nonlinear Langmuir wave [10].

Although type III solar burst characteristics have been measured for more than thirty years, it is important to be able to perform controlled experiments. An electron beam has been injected into the interplanetary plasma from a satellite [16]. However, in this experiment only emission at ω_{pe} was observed. It is only recently, with the availability of large size plasma devices, that laboratory simulations of second harmonic emission have been performed. In these experiments a single electron beam [17, 18], or two oppositely-propagating electron beams [19] are injected into the plasma. In the latter case, second harmonic emission results from the coupling of the two antiparallel propagating Langmuir waves which are excited by the two electron beams. The single electron beam experiments [17, 18] have more similarity to the actual astrophysical situation. In the experiment of Cheung et al. [17], a small diameter (beam diameter: 4 cm), cold beam was injected into a large size plasma. The beam had a density n_b/n_o of less than 3% and an energy E_b of up to 1 keV. Second and third harmonic emissions were observed. The ponderomotive force of the Langmuir waves caused a density depression of up to 20%.

In this paper, we would like to report on an experimental investigation of nonlinear effects associated with strong Langmuir turbulence. Preliminary results on second harmonic emission have been reported elsewhere [18]. The paper is organized as follows. The experimental arrangement and the diagnostics will be presented in section II. Section III is devoted to the second harmonic emission and density depression measurement. The results will be discussed in section IV.

2. EXPERIMENTAL ARRANGEMENT

The experiment is performed in a large plasma device (Fig. 1) (diameter: 2m, length: 3m). The base pressure in the device is 5×10^{-7} Torr. A steady state argon plasma is created by a discharge from 224 tungsten filaments. The bias voltage on the filaments is 60V and the argon filling pressure is 2×10^{-4} Torr. The plasma density n_o is $1.5 - 2 \times 10^{10}$ cm^{-3}, corresponding to a plasma frequency f_{pe} of 1.1 - 1.27 GHz. By adjusting the filament emission current a flat density profile was obtained in the region between the electron beam source and the microwave horn.

An electron beam is injected into the plasma from a barium-oxide coated cathode. The cathode diameter is 30 cm. It consists of sixteen strips of 1 mm thick nickel coated with BaO. The nickel strips are directly heated by the Joule effect. A high voltage (up to 3 kV) is applied to the cathode through a simple R-C current ($C \simeq .4$ μF, $R = 10\Omega$) which is triggered by a spark gap. The temporal evolution of the beam current and voltage are monitored. Typical maximum current is 20 A which lasts for about 10 μs and then decays to zero in 70 μs. The beam is guided by a weak axial homogeneous magnetic field (B_o: 2-5 Gauss, corresponding to an electron cyclotron frequency f_{ce} of 6-14 MHz). Taking for the diameter of the electron beam a value of 30 cm, the ratio of the beam density n_b to the plasma density n_o is of the order of $2 \cdot 10^{-3}$.

The steady state plasma density and the density fluctuations were monitored with movable Langmuir probes. During the electron beam injection, however, the plasma potential changes. Since this effect may influence electrical probe measurements, microwave interferometry was used as a complementary means to measure density variations. Initially, a 10 GHz microwave interferometer was installed to check whether ionization occurred during the beam injection. The system, which used standard X-band horns (beam divergence: 30° half width at half power), did not allow the measurement of small scale density variations. It was therefore replaced by a 10 GHz Lecher wire interferometer [20] (Fig. 1). The Lecher wire interferometer is a classical microwave interferometer where the microwave propagation in the plasma is guided by a two-conductor transmission line. The two conductors of the Lecher line consist of constantan wire (having a diameter of 0.3 mm, and a separation of 2.5 mm) with an oxide coating which prevents the drawing of current from the plasma. The line is impedance matched to the X-band waveguide. The Lecher wire interferometer is sensitive to a change of the dielectric constant of the medium in a cylindrical region of 3 mm diameter centred in the middle of the two wires. The spatial resolution of the interferometer in the direction perpendicular to the wires is therefore approximately 3 mm. The measured density fluctuation is, of course, averaged over the length of the wire. Two lengths were used: 60 cm and 30 cm, the latter one corresponding to the cathode diameter. For both interferometers (the one using horns and the other the Lecher wire), care has been taken to avoid any electrostatic coupling on the detection diodes during the beam injection. The reference arm and the arm crossing the plasma, which are connected

to the ground of the vacuum vessel, are galvanically decoupled from the magic Tee and diodes.

Microwave emission from the plasma is collected by a pyramidal horn inside the plasma. The horn and the waveguide to coaxial coupling section has a cut-off frequency of 1.5 GHz, preventing the measurement of radiation emitted at the plasma frequency. Time-resolved frequency spectra were obtained either directly from a spectrum analyser or from a heterodyning system. In the latter case, the signal is first filtered by a YIG preselector, which has a 3 db attenuation bandwidth of 50 MHz, amplified by a low noise 30 db gain amplifier. It is then converted to a fixed IF of 100 MHz by mixing with a local oscillator. The IF is detected by a low frequency spectrum analyser tuned to 100 MHz. The frequency response of both detection systems is flat within 1 db in the frequency range of 1.9 GHz to 3.3 GHz. The time resolution of the first method is, however, limited to 100 μs by the 10 kHz video filter of the spectrum analyser. The heterodyning method, which has a better signal to noise ratio, does not require the use of a video filter and has a time constant of 2 μs.

3. EXPERIMENTAL RESULTS

Without the injection of the energetic beam, electromagnetic radiation emission at the second harmonic is below the noise level of the detection system (noise power level: -105 dbm). Emission at the plasma frequency does not occur since the plasma is uniform [21]. This

measurement shows that the ionizing electrons from the filaments (E_b = 60 eV, $n_b/n_o = 10^{-4}$) do not excite a sufficiently high level of Langmuir turbulence to reach the strong turbulence regime.

When a high energy electron beam (E_b > 1 keV) is injected into the plasma, a strong increase of the power of the electromagnetic waves emitted at frequencies around twice the value of the original plasma frequency f_{pe} was observed. This increase amounts to 60 db compared to the steady-state level of the noise. Figure 2 shows the frequency spectrum of the electromagnetic waves in the range of 1.6 - 3.2 GHz at a time 4 μs after the beam injection. The beam energy is 2 keV. One notes a very strong increase (around 60 db) at frequencies around 2.2 GHz. The emission at frequencies around 2.2 GHz is identified as an emission at the second harmonic of the plasma frequency ($f_{pe} \approx$ 1.19 GHz) and not as an emission at the plasma frequency [21, 22] corresponding to a four-fold increase of the density due to ionization by the beam. We rule out the latter interpretation since both probe measurement and the microwave interferometry show that in the first 10 μs after the beam injection the plasma density does not change appreciably for the experimental values of neutral pressure and pulse length used. In fact, we found that working at higher neutral pressure (which yields a higher value of the plasma frequency and would allow a measurement of both the fundamental and second harmonic emission with the present horn), or longer pulse length (which would make time-resolved measurements easier), leads to significant ionization by the beam, and thus complicates the identification of the frequency of the emitted waves.

The ratio of the second harmonic to the fundamental frequency has been determined by changing the plasma density. Figure 3 shows this ratio to be 2(± .2). The experimental results of figure 3 were obtained from measurements for different beam energy for which second harmonic emission occurs. The second harmonic frequency is identified as the frequency where the maximum increase in power occurs.

Figure 4 shows the time evolution of the power emitted at 2.2 GHz. The experimental conditions are the same as for figure 2. It can be seen that 20 μs after the beginning of the injection the enhancement has decreased from 55 db to 30 db and is negligible at 50 μs. This behaviour correlates with the time evolution of the beam characteristics. After 20 μs, the beam current and voltage have dropped to half of their initial value and at 50 μs the beam energy was below 500 eV, which is a threshold value for second harmonic emission.

An important characteristic of the phenomena is the dependence of the power emitted at the second harmonic on the beam energy. The microwave detection system was tuned to the frequency corresponding to maximum enhancement (f = 2.2 GHz) and measurements taken at 4 μs. No significant emission at the second harmonic occurs for E_b below 500 eV (Fig. 5). Significant increases (30 - 50 db) of the power emitted at the second harmonic occur when E_b exceeds this value. The accuracy limit in the determination of the power of the emitted electromagnetic waves and the relatively small energy range covered in the experiment do not allow us to state whether the experimental points

could best be fitted by a linear E_b or quadratic E_b^2 relation. These measurements, however, help to clarify the time behaviour of the increase in power shown in figure 4. At 20 μs, the beam voltage is 1000 V, for which figure 5 shows that the increase of the power emitted drops to approximately 35 db. Below an energy of 500 eV, corresponding to time greater than 50 μs, no second harmonic emission occurs.

We now turn to the second important point predicted by strong Langmuir turbulence, namely the formation of a density depression due to the ponderomotive force of large amplitude Langmuir waves. Local density variations were measured with a Langmuir probe biased at -100 V or at +10 V to collect either the ion or the electron saturation current. In both cases, the saturation current measured indicates a density decrease ($\delta n/n_o \simeq$ 20 - 30%) during the first five microseconds (Fig. 6). Although electrical probe measurements may be perturbed during the energetic electron beam injection, at which time the plasma potential changes by about 10 V and sheath rectification of the large amplitude Langmuir waves excited by the beam occurs, the insensitivity of the results with respect to the probe bias indicates that the measurements are, at least qualitatively, correct. Note also that the use of an electrical probe is current in similar experimental situations [23]. The probe measurements are confirmed by the results obtained using the Lecher wire interferometer. The transverse size of the density depression (i.e. in the direction perpendicular to the beam velocity) is roughly equal to the cathode diameter (30 cm). This result was inferred from measurements of the density depression using the Lecher wire interferometer operating with two different lengths of

transmission line, 60 cm and 30 cm. In both cases, the transmission line is symmetric with respect to the centre of the cathode. Using a length of 30 cm it was found that the line average of the density decrease $\delta n/n_o$ is twice as large as that obtained with a length of 60 cm. This indicates that for radii greater than the radius of the cathode, $\delta n/n_o$ is approximately zero.

The variation of $\delta n/n_o$ with respect to the beam voltage is shown in figure 7. Results from the Lecher wire interferometer clearly indicate that for E_b below 1 keV, no density depression is formed. Recall that a similar conclusion was obtained for the second harmonic emission (Fig. 5).

4. DISCUSSION

The theory of strong Langmuir turbulence has often been invoked to explain the second harmonic emission of type III solar bursts. Since our experimental conditions differ considerably from the solar or interplanetary plasma conditions (10 keV$<E_b<$100 keV, $n_o=40cm^{-3}$, $n_b/n_o = 5 \times 10^{-4}$) for which calculations have been performed, let us verify whether the strong Langmuir turbulence theory may be applied. The main criterion is the value of the energy W_r of the waves in resonance with the beam compared with $(k\lambda_{De})^2$, where k is a typical wavenumber of the excited wave ($k = \omega_{pe}/v_b$) and λ_{De} the Debye length. Strong Langmuir turbulence effects occur when W_r reaches values comparable to $(k\lambda_{De})^2$ [14]:

$$W_r = E^2/8\pi\, n_o k_B T_e \geq (k\lambda_{De})^2. \qquad (1)$$

For a typical experimental condition (E_b = 2000 eV), $k\lambda_{De}$ is 1.7×10^{-2} and the threshold value for W_r is given by

$$W_r > 2.8 \times 10^{-4} \tag{2}$$

Let us now consider the linear beam plasma instability. The growth rate for a cold beam is given by [24]:

$$\frac{\gamma}{\omega_{pe}} = \frac{\sqrt{3}}{2}\left(\frac{n_b}{n_o}\right)^{1/3} \simeq .09 \tag{3}$$

Assuming the Langmuir waves are destabilized from the thermal value, the initial value of W_r is of the order of 10^{-8}. It would then take a time t given by

$$\omega_{pe} t \simeq \frac{\ell n\ 10^4}{.09} \simeq 100 \tag{4}$$

to reach the threshold value. This time (t = 90 ns) is very short compared to the pulse length (≈ 10 μs). Subsequent evolution of the wave is then dominated by nonlinear effects such as the collapse of Langmuir waves.

Papadopoulos [7] has also determined the domain of parameters for which the strong Langmuir turbulence theory is valid (Fig. 8). The parameters of our experiment lie almost entirely within the region where the strong Langmuir turbulence theory is applicable. Figure 8 also shows that for low beam energy (around 200 eV) quasi-linear effects would dominate. A beam energy of 500 eV was found to be a threshold for second harmonic emission in our experiment.

Our experiment has provided evidence of some of the features predicted by the strong Langmuir turbulence theory. The spontaneous formation of a density depression caused by the ponderomotive force due to the collapse of Langmuir waves has been observed in our experiment. Similar measurements have been reported by Cheung et al. [17] in a laboratory device and by Gurnett et al. [26] in the Jovian plasma. The amplitude of the density depression $\delta n/n_o$ yields an estimate of the peak field amplitude [23, 25]:

$$\frac{\delta n}{n_o} = \frac{E^2}{8\pi n_o k_B T_e} \quad . \tag{5}$$

The measured value of $\delta n/n_o$ = 10 - 30% corresponds to a peak value of the electric field of $E^2/(8\pi n_o k_B T_e) \approx .1 - .3$.

A second point of importance is the dependence of the power emitted at the second harmonic with respect to the Langmuir wave W_r energy. A linear dependence is predicted by Papadopoulos and Freund's theory [10] whereas an upperbound proportional to W_r was found by Goldman et al. [13]. In our experiment the increase of W_r with E_b was measured (Fig. 9). A linear relationship was found. Consequently, the figure (5) gives a relation between the power emitted at $2\,\omega_{pe}$ and the Langmuir wave energy. The present experimental evidence is insufficient to give a definite answer to this problem and measurements using larger values of beam energy are necessary.

Finally we would like to comment on the problem of beam stabilization. It is well known that the quasi-linear effect with its very large energy transfer rate η_{QL} between the beam and the excited waves ($\eta_{QL} = 1/3$) leads to very fast beam stabilization. The distance over which the plateau formation occurs is given by [27]

$$L_{QL} = 0.2(n_o/n_b)\ (v^2_{the}/\omega_{pe} v_b)\ \Lambda \qquad (6)$$

where v_{the} is the thermal velocity and Λ the Coulomb logarithm. Using the values appropriate to our experimental conditions, L_{QL} is of the order of 1 cm. Experimentally, we have observed a density depression at distances much further from the cathode: for example, the Lecher wire interferometer is located 60 cm from the cathode. If the beam was thermalized by the quasi-linear effect, large amplitude waves would not exist so far from the cathode and no density depression would have been formed.

5. CONCLUSION

We have presented experimental evidence of second harmonic radiation in a beam plasma system. Density depressions have also been observed unambigously. Qualitative agreement exists with results from the theory of strong Langmuir turbulence. Future experimental work will be performed in the beam parameter regime of type III solar bursts.

ACKNOWLEDGEMENT

We wish to acknowledge discussions with Dr. Ch. Hollenstein, M.L. Sawley, J. Vaclavik and Prof. K. Papadopoulos. This work is supported by the Swiss National Science Foundation, the Ecole Polytechnique Fédérale de Lausanne and Euratom.

REFERENCES

[1] S.A. Kaplan, S.B. Pikel'ner and V.N. Tsytovitch, Phys. Lett. 15C, 1 (1974).

[2] D.F. Smith, Adv. Astron. Astrophys. 7, 147 (1970).

[3] J.P. Wild and S.F. Smerd, Ann. Rev. Astron. Astrophys. 10, 153 (1972).

[4] M.V. Goldman, Preprint No RPP 2521, CSIRO (Australia) (1981).

[5] R.P. Lin, Space Science Rev. 16, 189 (1974).

[6] S.R. Kaplan and V.N. Tsytovitch in Plasma Astrophysics, ed. by Pergamon Press (1973) - Chapter II, p. 101 - 150.

[7] K. Papadopoulos, Phys. Fluids 18, 1769 (1975).

[8] H.L. Rowland and K. Papadopoulos, Phys. Rev. Lett. 39, 1276 (1977).

[9] D.R. Nicholson, M.V. Goldman, P. Hoyng and J.C. Weathershall, Astrophys. J. 223, 605 (1978).

[10] K. Papadopoulos and H.P. Freund, Geophys. Rev. Lett. 5, 881 (1978).

References (cont'd)

[11] D.F. Smith and D.R. Nicholson in Wave instabilities in space plasmas, ed. by Palmadesso and K. Papadopoulos (D. Reidel Publishing Co. 1979), p. 225.

[12] M.L. Goldstein and K. Papadopoulos, ibid. p. 245.

[13] M.V. Goldman, G.F. Reiter and D.R. Nicholson, Phys. Fluids 23, 208 (1980).

[14] H.L. Rowland, Phys. Fluids 23, 508 (1980).

[15] B. Hafizi, J.C. Weatherhall, M.V. Goldman and D.R. Nicholson, Phys. Fluids 25, 392 (1982).

[16] R.A. Hendrickson, R.W. McEntire and J.R. Winckler, Nature 230, 564 (1971).

[17] P.Y. Cheung, A.Y. Wong, C.B. Darrow and S.J. Qian, Phys. Rev. Lett. 48, 1348 (1982).

[18] M. Schneider and M.Q. Tran to be published in Phys. Lett. A.

[19] J. Santoru, P. Leung and A.Y. Wong in Physics of Auroral Arc Formation, S.I. Akasofu and J.R. Kan editors (AGU 1981), p. 387.

References (cont'd)

[20] W. Makios, Rev. Sci. Instr. 38, 352 (1967).

[21] R.W. Means, L. Muschietti, M.Q. Tran and J. Vaclavik, Phys. Fluids 24, 2197 (1981).

[22] L.D. Bollinger and M. Böhmer, Phys. Rev. Lett. 26, 535 (1971).

[23] P. Leung, M.Q. Tran and A.Y. Wong to be published in Plasma Physics.

[24] S.A. Self, M.M. Shoucri and F.W. Crawford, J. Appl. Phys. 42, 704 (1971).

[25] A.Y. Wong and B.H. Quon, Phys. Rev. Lett. 34, 1499 (1975).

[26] D.A. Gurnett, J.E. Maggs, D.L. Gallagher, W.S. Kurth and F.L. Scarf, J. Geophys. Res. 86, 8833 (1981).

[27] A.A. Vedenov and D.D. Ryutov in Reviews of Plasma Physics Vol. 6, ed. by M.A. Leontovitch (1975), p. 12.

FIGURE CAPTIONS

Figure 1 The experimental device. The size of the plasma volume is 3 m length and 2 m diameter. A pyramidal horn is used to detect the electromagnetic wave. A Lecher wire X-band interferometer is used to detect small scale density perturbation.

Figure 2 Frequency of the electromagnetic waves emitted 4 μs after the beam injection. The plasma frequency is equal to 1.19 GHz. The peak around 2.2 GHz corresponds to the second harmonic.

Figure 3 Ratio of the second harmonic to the fundamental frequency f_{pe} as a function of f_{pe}.

Figure 4 Time evolution of the power emitted at the second harmonic. The electromagnetic wave frequency is 2.2 GHz.

Figure 5 Dependence of the power emitted at the second harmonic on the beam energy. The measurements were performed at a frequency of 2.2 GHz.

Figure 6 Density depression measured by a Langmuir probe collecting electron I_e and ion I_i saturation currents.

Figures (cont'd)

Figure 7 Dependence of the density depression $\delta n/n_o$ on the beam energy E_b. ○ are values obtained using a Langmuir probe biased at +10 V, while ● are values obtained from the Lecher wire interferometer.

Figure 8 Domain of the parameters n_b/n_o and E_b/k_BT_e where strong Langmuir turbulence (NL) and quasi-linear (QL) theories are applicable [Ref. 7]. The region corresponding to the parameters of the present experiment is denoted by (E).

Figure 9 Variation of the power at ω_{pe}, as measured with a Langmuir probe at floating potential, with the beam energy E_b.

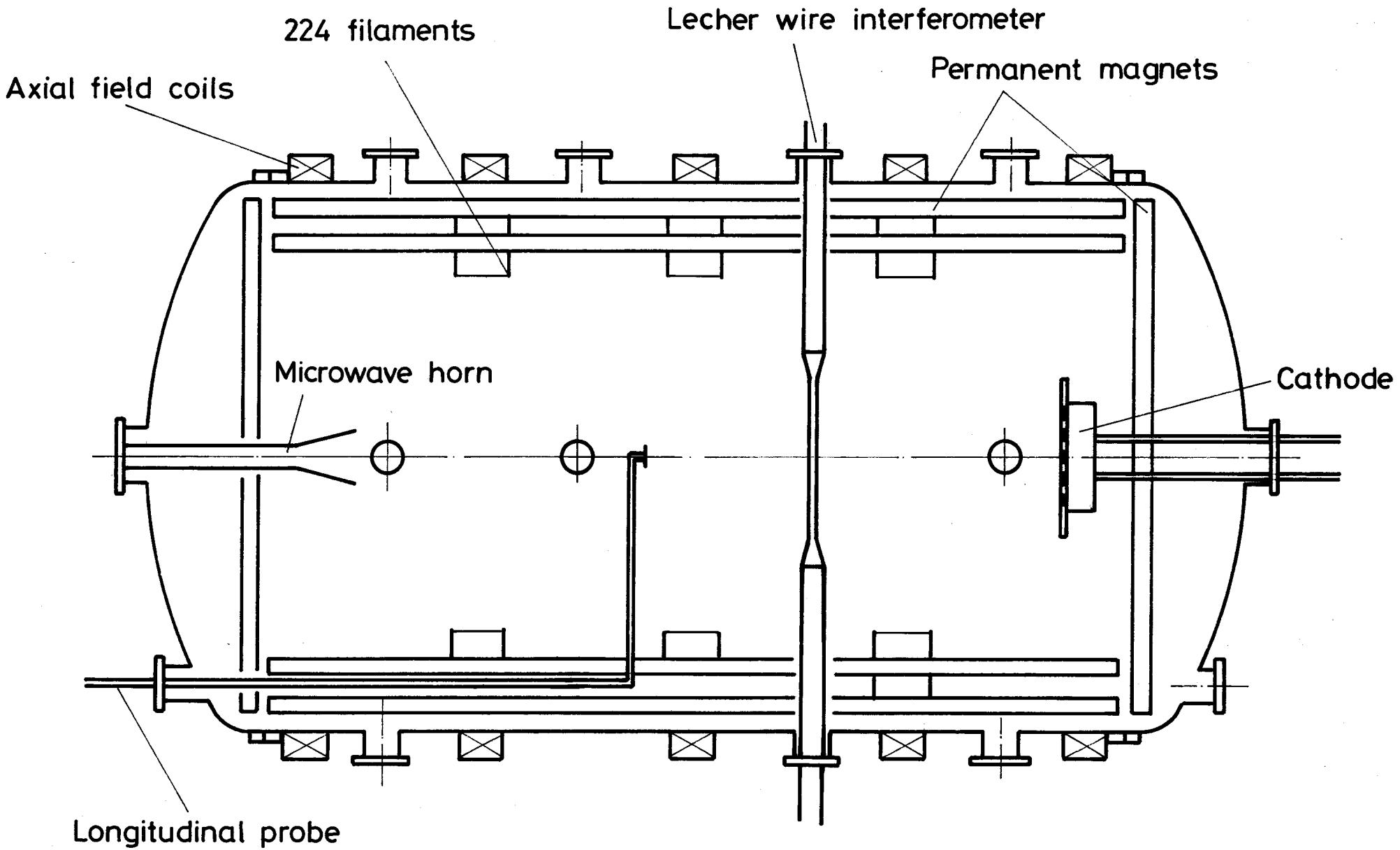
224 filaments
Lecher wire interferometer
Axial field coils
Permanent magnets
Microwave horn
Cathode
Longitudinal probe

Fig. 1

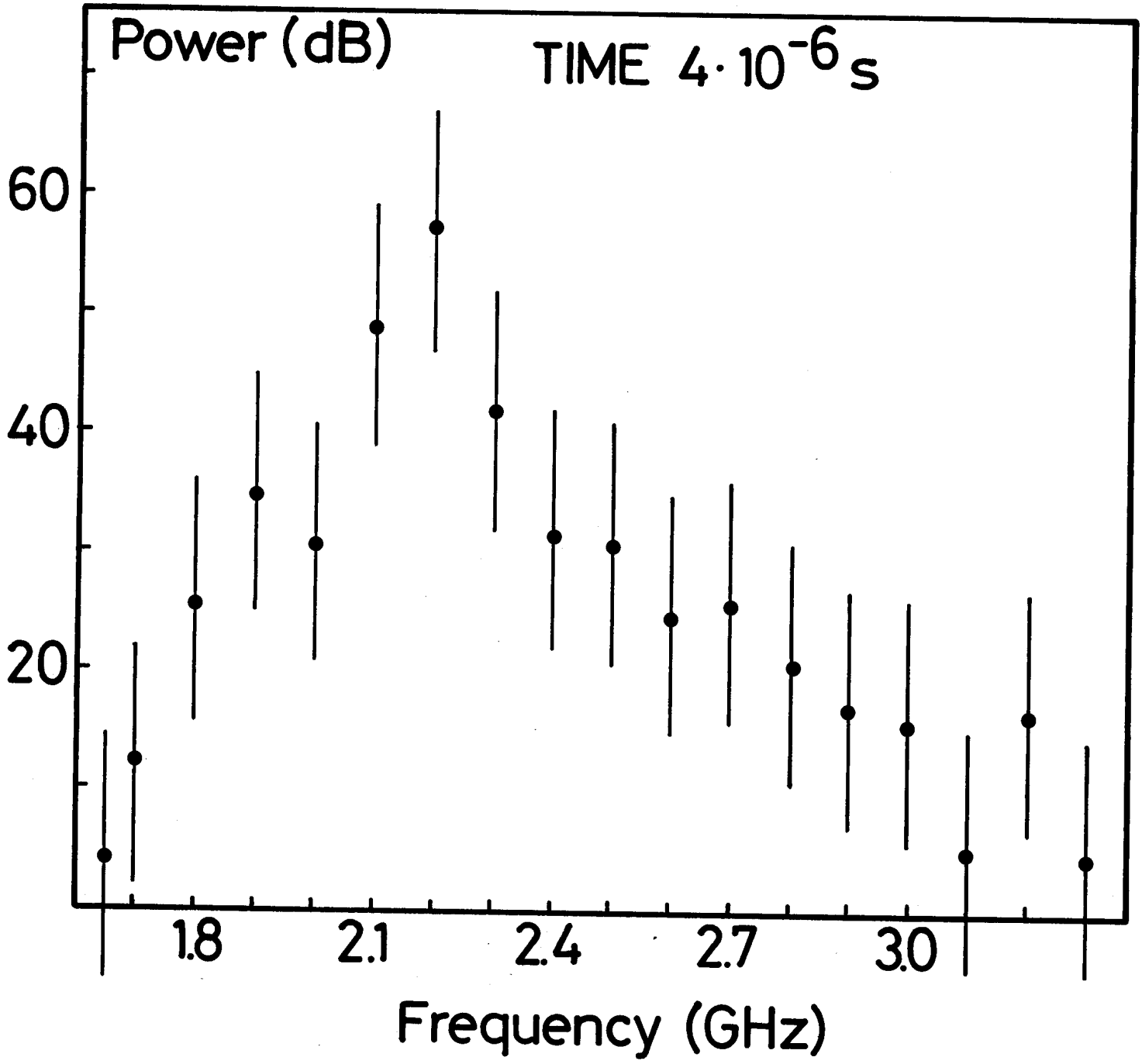

Fig. 2

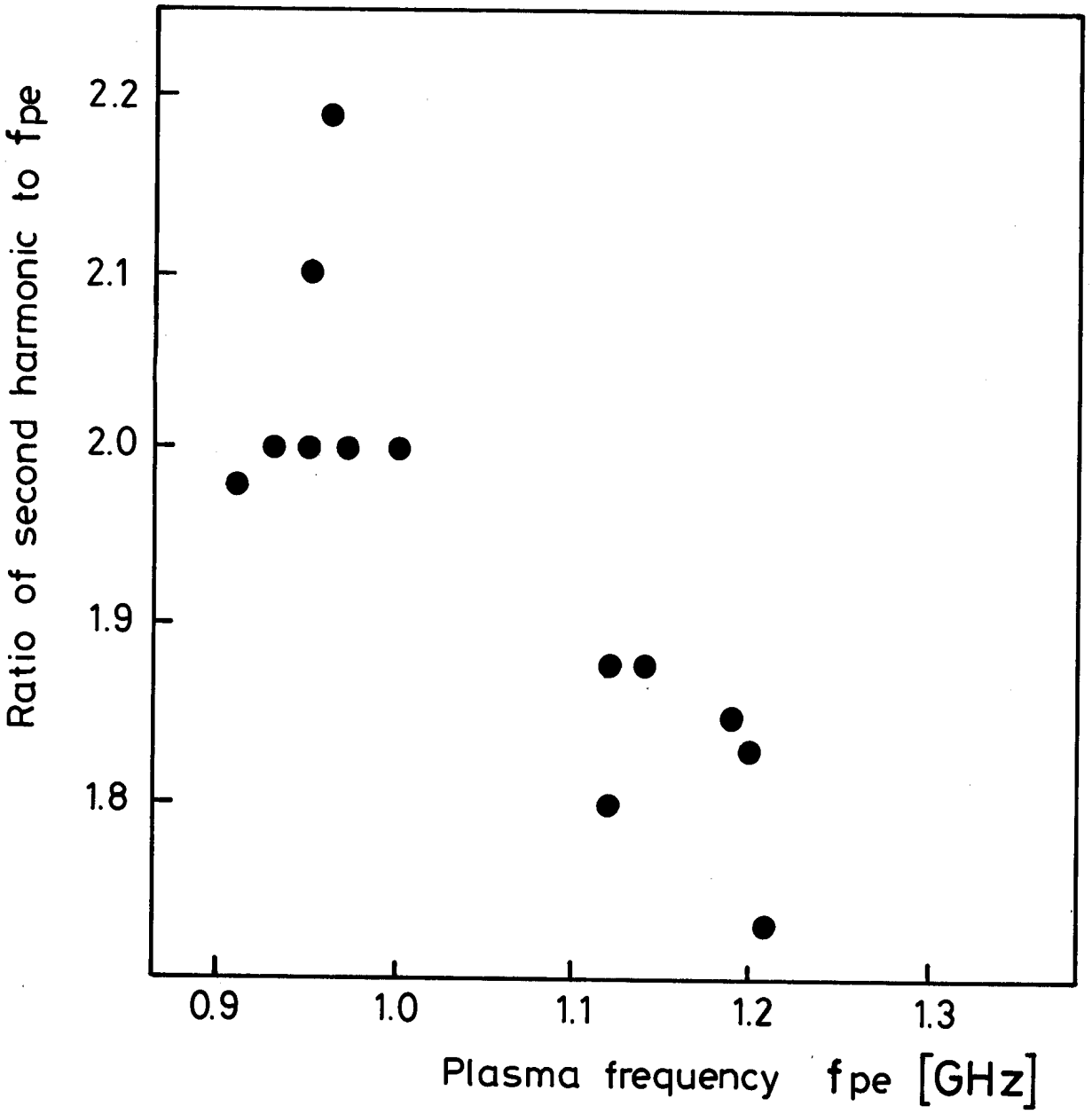
Ratio of second harmonic to fpe
2.2
2.1
2.0
1.9
1.8
0.9
1.0
1.1
1.2
1.3
Plasma frequency fpe [GHz]

Fig. 3

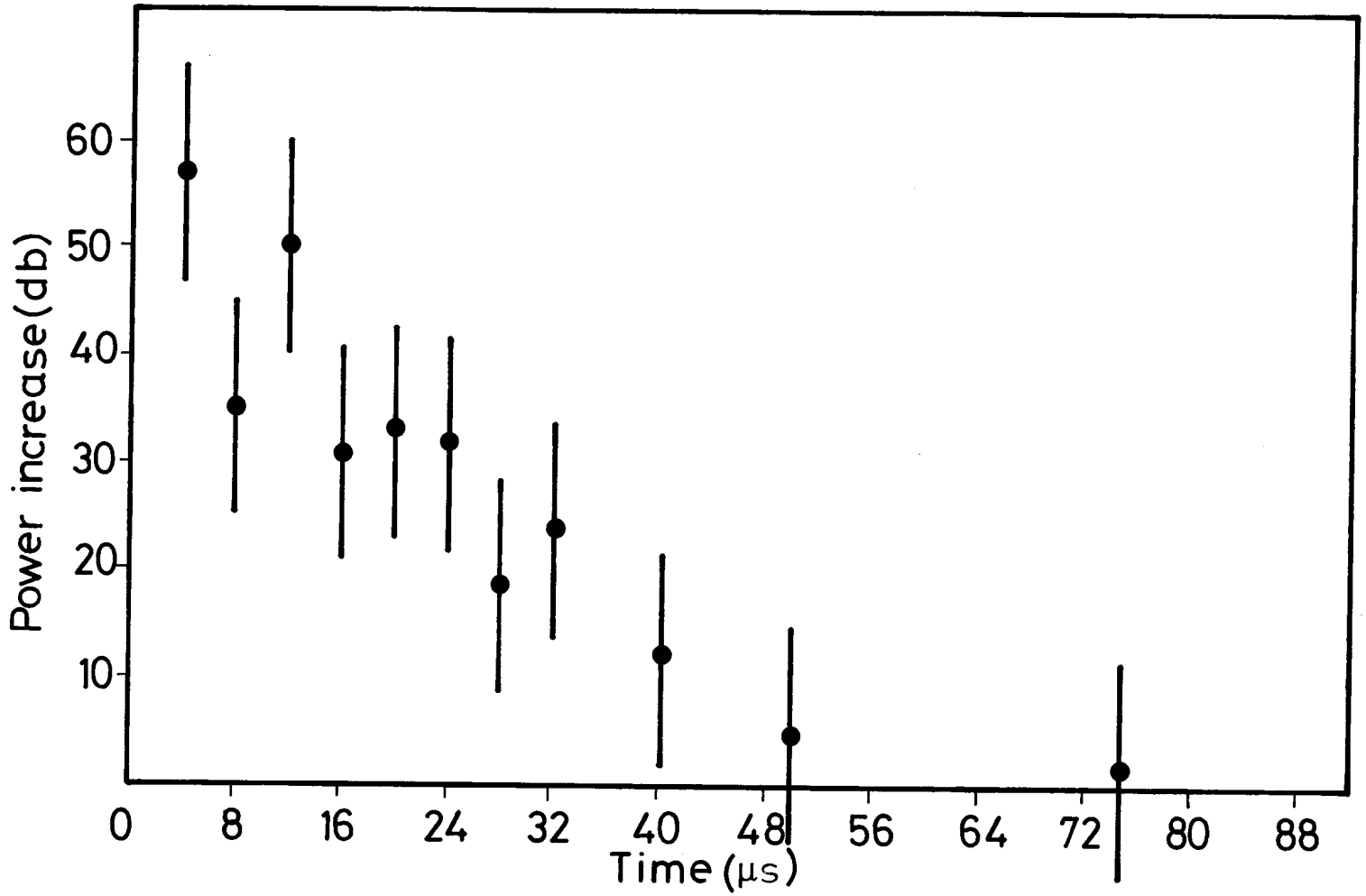
Power increase (db)
60
50
40
30
20
10
0
8
16
24
32
40
48
56
64
72
80
88
Time (μs)

Fig. 4

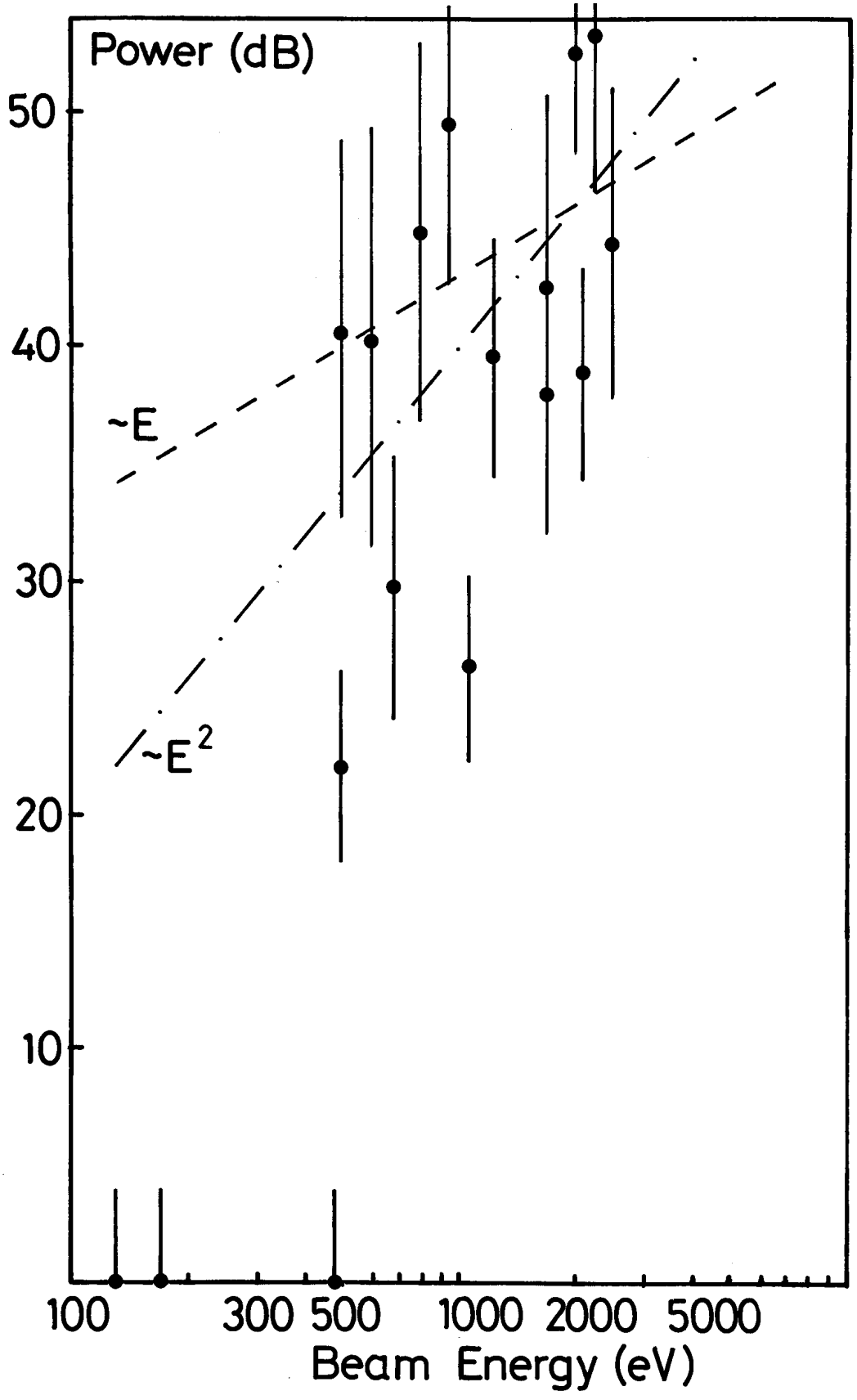
Power (dB)
50
40
30
20
10
~E
~E²
100
300
500
1000
2000
5000
Beam Energy (eV)

Fig. 5

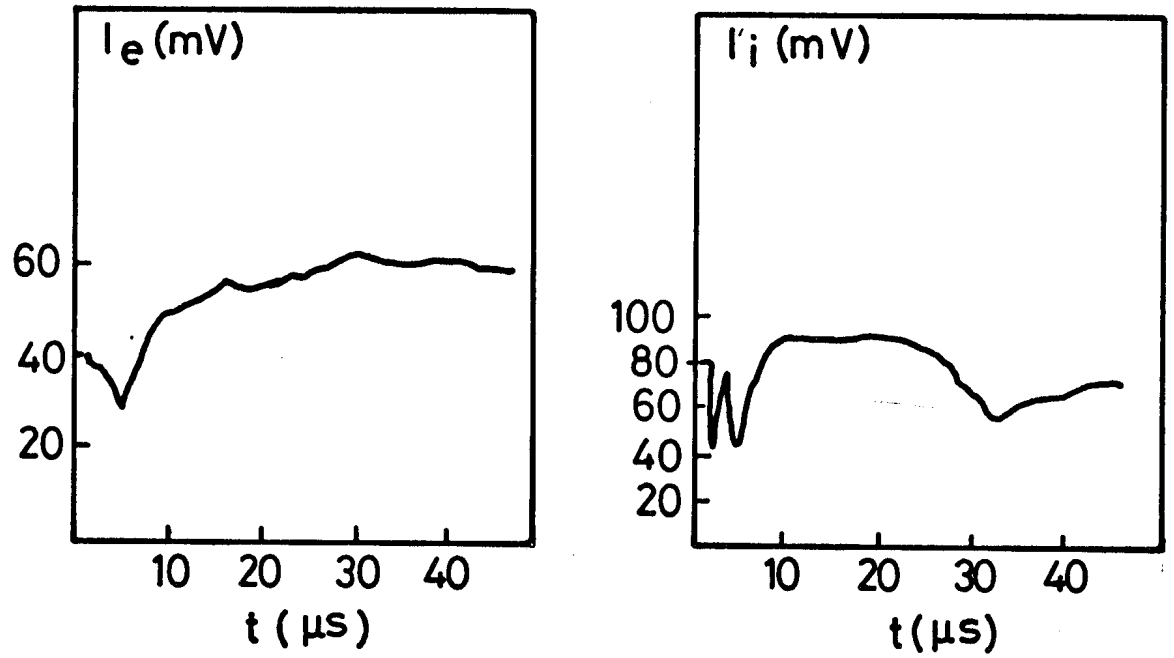

Fig. 6

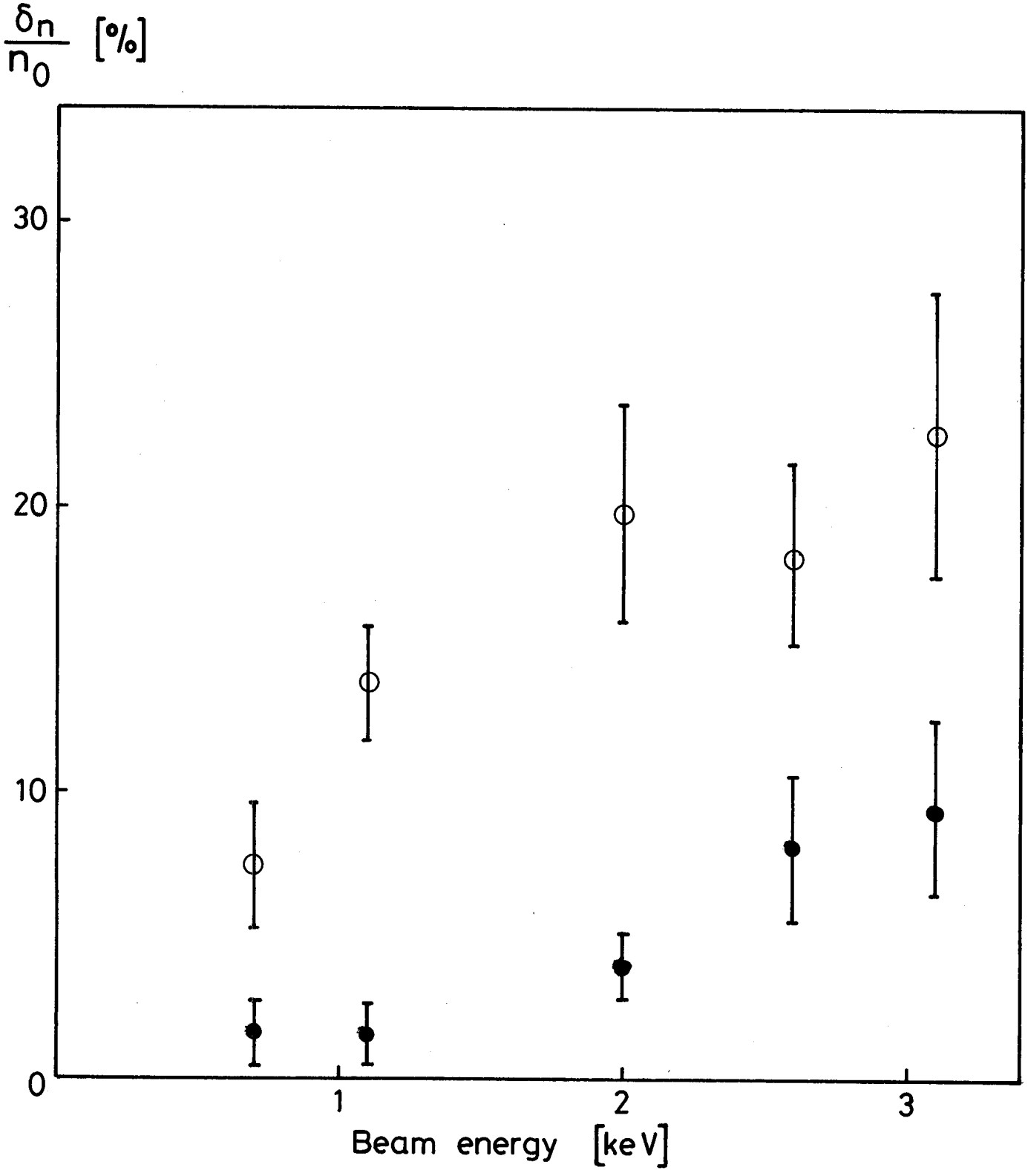

Fig. 7

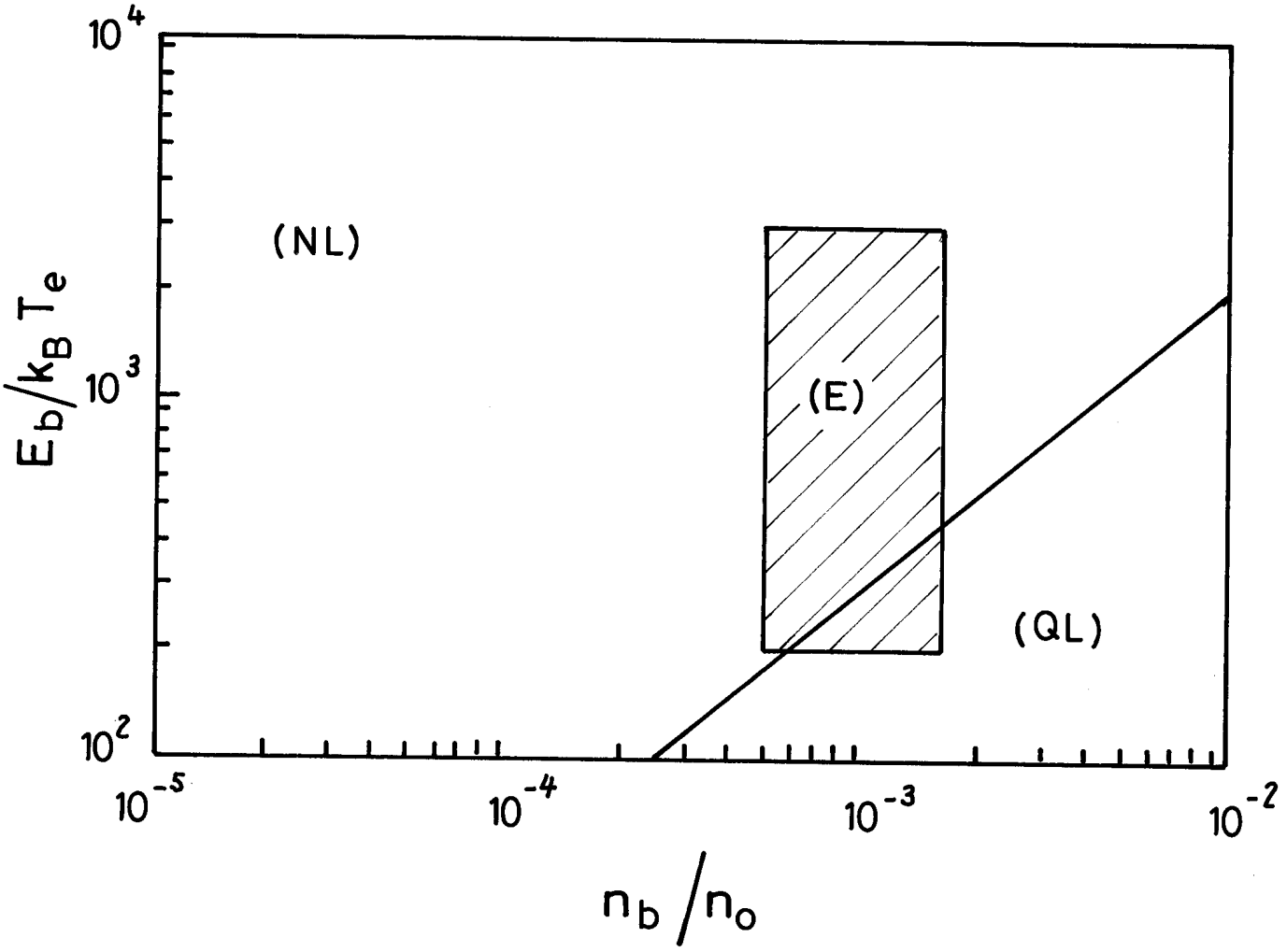

Fig. 8

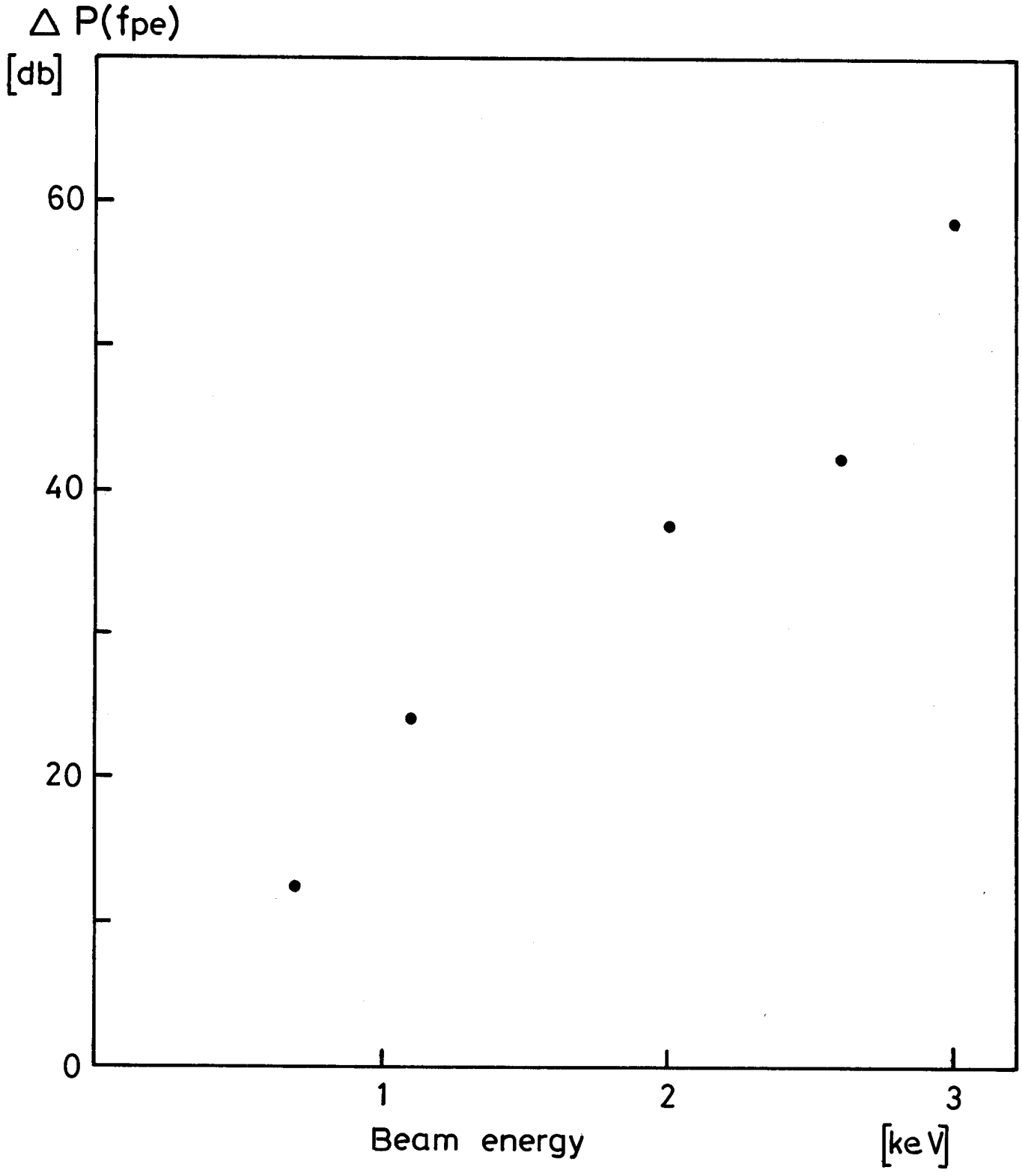

Fig. 9